LETTERS

Phase-contrast X-ray microtomography links Cretaceous seeds with Gnetales and Bennettitales

Else Marie Friis[1], Peter R. Crane[2], Kaj Raunsgaard Pedersen[3], Stefan Bengtson[1], Philip C. J. Donoghue[4], Guido W. Grimm[5] & Marco Stampanoni[6]

Over the past 25 years the discovery and study of Cretaceous plant mesofossils has yielded diverse and exquisitely preserved fossil flowers that have revolutionized our knowledge of early angiosperms[1], but remains of other seed plants in the same mesofossil assemblages[2,3] have so far received little attention. These fossils, typically only a few millimetres long, have often been charred in natural fires and preserve both three-dimensional morphology and cellular detail. Here we use phase-contrast-enhanced synchrotron-radiation X-ray tomographic microscopy to clarify the structure of small charcoalified gymnosperm seeds from the Early Cretaceous of Portugal and North America. The new information links these seeds to Gnetales (including Erdtmanithecales, a putatively closely related fossil group[2]), and to Bennettitales—important extinct Mesozoic seed plants with cycad-like leaves and flower-like reproductive structures. The results suggest that the distinctive seed architecture of Gnetales, Erdtmanithecales and Bennettitales defines a clade containing these taxa. This has significant consequences for hypotheses of seed plant phylogeny by providing support for key elements of the controversial anthophyte hypothesis, which links angiosperms, Bennettitales and Gnetales.

Relationships among extant seed plants (cycads, *Ginkgo*, conifers, Gnetales and angiosperms) remain controversial[4,5], but because these are only a small sample of the total diversity in the seed plant clade, new information on extinct seed plants is likely to be crucial to resolve the current impasse[4–6]. Here we describe new material from a diverse collection of gymnospermous seeds that all have a similar basic structure. These seeds have excellent cellular preservation and are widespread in the Early Cretaceous mesofossil assemblages that we have examined from Portugal and eastern North America. They have been studied previously with standard techniques, but synchrotron radiation X-ray tomographic microscopy, which has been applied successfully to study various microfossils without the need for destructive analysis[7–9], provides a more complete understanding of their complex internal structure. For our material, attenuation-based synchrotron-radiation X-ray tomography (SRXTM) does not provide sufficient contrast because of the low absorption of the charcoalified cell walls, whereas phase-contrast X-ray tomographic microscopy (PCXTM, see Methods) provides high resolution at the cellular level.

The fossil seeds are about 0.5–1.8-mm long, obovate to obtriangular or elliptical in longitudinal outline, and distinctly four-angled in transverse section (Figs 1, 2). At the apex there is a central projection, which in some seeds is surrounded by four, pointed, tepal-like structures that project upwards from the four angles. The seeds have a broad stalk, but in most specimens it is broken off. The fossils superficially resemble angiosperm flowers[10], but have also been compared with seeds of Gnetales and Erdtmanithecales[3,10]. PCXTM establishes that the fossils are small seeds comprised of two distinctly different layers surrounding the nucellus: an inner thin, membranous, integument, formed by thin-walled cells, and a robust outer, sclerenchymatous, seed envelope that completely encloses the integument except for the micropylar opening.

The integument is slightly shrunken in all specimens examined but there is no well-developed nucellus membrane or megaspore membrane. The integument and outer envelope are free for their full length and are attached only by a broad connection at the base (Fig. 1, left panel). The integument is free from the nucellus in its upper part and tapers into a long, narrow micropylar tube that is circular in transverse section. The micropylar canal is open towards the apex, and the integument in this region consists of one or two layers of small cells (Fig. 1, CS1). In the middle part and towards the base, the micropylar canal is closed by expanded tissue of the integument, which, at this level, consists of several cell layers. In particular, the cells of the inner epidermis are expanded radially to form a prominent ring that closes the micropylar canal (Fig. 1, CS2). At the base of the micropyle, the integument opens again, but the inner lining is irregular and the inner cells are broken down (Fig. 1, CS3).

The envelope is mainly composed of a hard sclerenchymatous tissue. At the apex this tissue forms a distinct, central projection around the micropylar tube formed by the integument. It also forms the protrusions that extend from the corners of the seed (Fig. 1a–d). In some seeds these merge proximally to form a ring-like structure (Fig. 1a); in others they are thinner and more discrete. There is considerable diversity in seed size and the form of the outer surface among this group of seeds.

The envelope has an inner layer of narrowly elongated sclerenchyma cells that are transversely aligned around the main body of the seed. Towards the apex these sclerenchyma cells are expanded radially (Figs 1d, 2c). The inner surface of the envelope is smooth and non-papillate, including around the micropyle (Figs 1d, 2c). The outer surface has irregular transverse ridges, which give the seed a wrinkled appearance (Figs 1b, c, 2a). The cells comprising this layer are elongated and aligned vertically. Occasional remains of parenchymatous tissues outside the wrinkled surface of the sclerenchyma layer suggest that the seed envelope had a thin, fleshy outer covering.

Only Gnetales (extant and extinct), Erdtmanithecales (extinct) and Bennettitales (extinct) are known to have seeds of this kind with an additional seed envelope and the integument extended into a long, narrow micropylar tube. In all three extant genera of Gnetales, the integument is thin and fused to the nucellus for most of its length. At the base, the fused integument is broadly attached and surrounded by one (*Ephedra*, *Welwitschia*) or two (*Gnetum*) envelopes, by which it is

[1]Departments of Palaeobotany and Palaeozoology, Swedish Museum of Natural History, SE-104 05 Stockholm, Sweden. [2]Department of the Geophysical Sciences, University of Chicago, Chicago, Illinois 60637, USA. [3]Department of Earth Sciences, University of Aarhus, DK-8000 Århus C, Denmark. [4]Department of Earth Sciences, University of Bristol, Bristol BS8 1RJ, UK. [5]Institute of Geosciences, Eberhard-Karls-University, D-72076 Tübingen, Germany. [6]Swiss Light Source, Paul Scherrer Institut, CH-5232 Villigen, Switzerland.

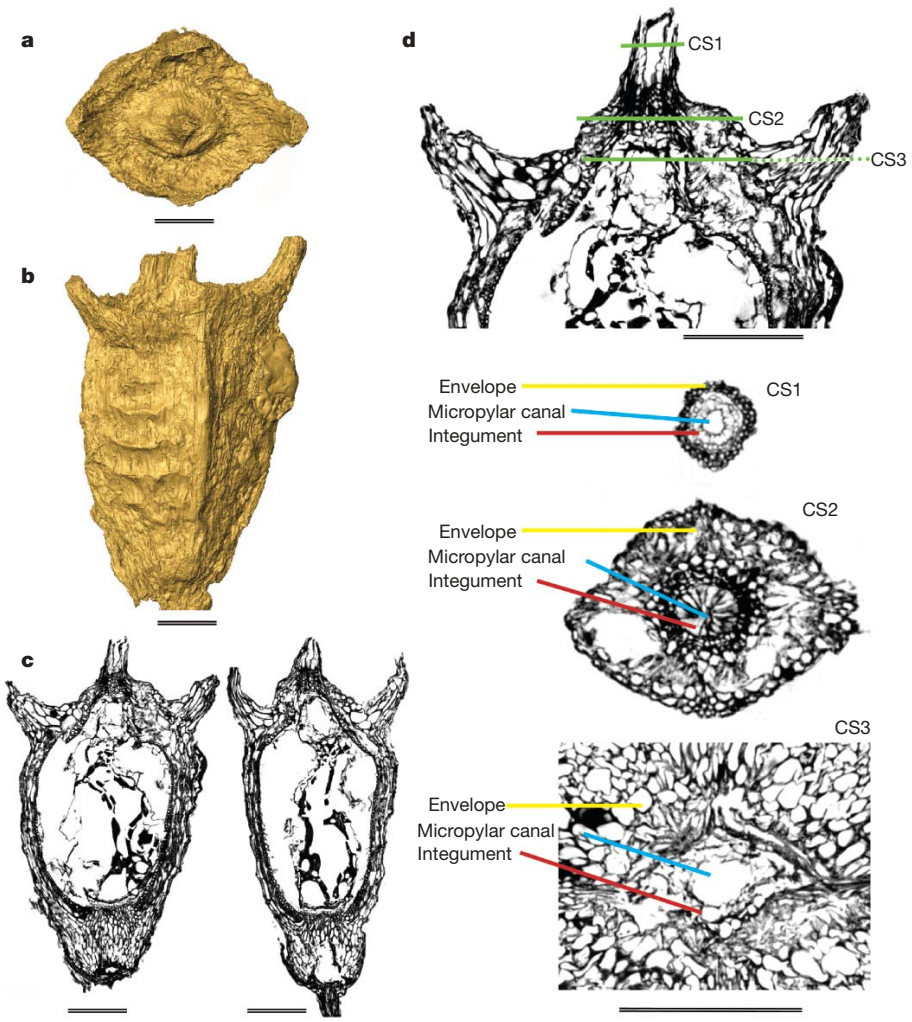

Figure 1 | Early Cretaceous (Barremian–Aptian) seed from Catefica, Portugal, with affinities to Gnetales and Bennettitales. S153152 (see Methods). **a**, **b**, Tomographic reconstructions of seed morphology in apical (**a**) and lateral (**b**) view showing quadrangular shape, micropylar protrusion and four apical extensions of the envelope. **c**, **d**, PCXTM images of internal structures. **c**, Longitudinal sections (perpendicular to each other) showing membranous inner tissues (megaspore membrane, nucellus and integument) surrounded by sclerenchymatous tissue of the envelope. **d**, Longitudinal section showing the micropylar area and position of transverse sections (CS1, open micropylar canal; CS2, closed canal; CS3, base of micropylar region). Scale bar in all figures, 200 μm (CS1, CS2 and CS3 share the same scale bar).

almost entirely enclosed. In *Ephedra*, cells lining the micropylar canal are small and uniform in size and shape. At maturity, the micropylar canal is closed by a hardened mucilaginous secretion[11]. In *Gnetum*, *Welwitschia* and the fossil seeds described here, the micropylar canal is open distally, but blocked in the middle and also proximally by a multicellular closing tissue formed by the expanded integument[12–14].

In *Ephedra* and *Gnetum*, the envelope surrounding the integument has an inner sclerenchymatous and an outer fleshy zone; in *Welwitschia*, this envelope forms a pronounced membranous wing; in extant *Ephedra*, the sclerenchymatous envelope is usually bisymmetric or sometimes triangular in cross-section. However, several Early Cretaceous *Ephedra* seeds (*E. portugallica* and *E. drewriensis*) have a four-parted envelope that is very similar to that of the fossil seeds described here[3]. Also similar to the charcoalified seeds, the surface of the sclerenchymatous zone in extant *Ephedra* (for example, *E. rhytidosperma*) and extinct ephedroid seeds is sometimes transversely ribbed[3,15]. However, seeds of *Ephedra* differ from the material described here in lacking the micropylar closing tissue and in having a distinct papillate inner lining on the outer envelope around the micropylar tube.

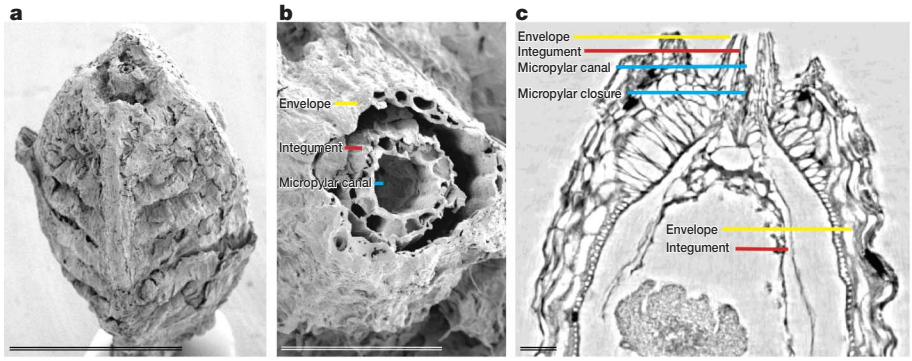

Figure 2 | Early Cretaceous (mid-Albian) seed from the Puddledock locality, USA, with affinities to Gnetales and Bennettitales. PP53361 (see Methods). **a**, **b**, Scanning electron microscope images of external morphology; oblique lateral view (**a**) showing the ribbed surface of the sclerenchymatous seed envelope and remains of the fleshy outer layer; scale bar, 500 μm; apical view (**b**) showing details of the micropylar extension with the seed envelope surrounding the integument and micropylar canal; scale bar, 50 μm. **c**, PCXTM image (longitudinal) of internal seed structures showing remains of the embryo sac and nucellus surrounded by thin integument and thick sclerenchymatous seed envelope; scale bar, 50 μm.

Seeds of Erdtmanithecales (*Erdtmanispermum*) from the earliest Cretaceous are very similar to those of *Ephedra*[2] and have a three-parted sclerenchymatous envelope, which is sometimes faintly ribbed externally. However, they differ from seeds of extant and extinct *Ephedra* by the presence of distinctive *Eucommiidites*-type pollen in the micropyle and by the lack of a papillate lining on the outer envelope around the micropylar tube. Pollen organs of Erdtmanithecales also differ from those of extant Gnetales. Unfortunately, in *Erdtmanispermum* seeds cellular details of the micropyle closure are not clear.

Seeds of Bennettitales are also small except for several Triassic forms[16,17]. In all cases the seeds are borne on stalks in conical to globose heads, between densely crowded interseminal scales. Dispersed seeds have never been recognized and, despite the excellent preservation of many petrified specimens, the organization of the seeds remains controversial. Bennettitalean seeds have been interpreted as having a single integument and no other additional coverings[18,19], or as having a thin integument surrounded by an additional envelope[16,17,20]. Interseminal scales have been interpreted as aborted ovules, and the entire ovulate structure has been considered to consist of naked seeds (fully developed and aborted) with no supporting structures[16,17,20].

Comparison of the charcoalified seeds from Portugal and North America with petrified seeds of Bennettitales from ovulate heads[18,19,21] reveals striking similarities. As in the charcoalified fossils, there is an outer layer with a sclerenchymatous and parenchymatous zone. In some species the sclerenchymatous layer is distinctly four- to five-angled in transverse section, in others it is five- or sometimes six-angled. The outer surface of the sclerenchymatous layer is irregularly ribbed in several taxa. Also, in *Cycadeoidea*, the sclerenchymatous layer often extends apically from the corners of the seed to form extensions that flank the micropylar area, as in the charcoalified fossil seeds (see Supplementary Information).

Petrified seeds of *Cycadeoidea morierei* show especially well-preserved cellular details that can be compared directly with the charcoalified fossils and seeds of Gnetales[12,13]. It is clear that the sclerenchyma layer in *C. morierei* surrounds a discrete micropylar tube with an inner epidermis of prominent radially expanded cells, which forms a ring around the open micropylar canal[21]. Towards the middle and base of the micropylar canal, closure is by a multicellular tissue, and at the base of the canal, disintegration of the central cells forms an irregular cavity[21]. The proliferated cells in the middle of the micropyle are identical to the closing tissue observed in *Gnetum* and *Welwitschia*[12]. The details revealed by PCXTM show that this layer is not a nucellar plug or part of the nucellus[18,19]. In *Cycadeoidea morierei*, there is a thin parenchymatous membrane inside the sclerenchymatous layer, which is similar to the integument seen in the charcoalified seeds and seeds of Gnetales.

On the basis of anatomical and positional similarities, we equate the sclerenchymatous layer in petrified seeds of Bennettitales to the very similar sclerenchymatous envelope that surrounds the integument in our charcoalified seeds. This outer envelope is also visible in some Bennettitales, preserved as compressions[16,17,20], *Erdtmanispermum*, *Ephedra* and *Welwitschia*, and *Gnetum* (middle layer). In Gnetales, this envelope is commonly interpreted as a pair of modified bracts[20]. The seed envelope in extinct Gnetales, as well as in *Erdtmanispermum*, Bennettitales and the charcoalified seeds, is also interpreted most straightforwardly as two or more bracts. This has profound implications for the morphological interpretation of bennettitalean 'flowers'—it suggests that the ovulate 'flowers' are an aggregation of strongly condensed bracteate reproductive axes, which opens up new possibilities for clarifying homologies with structures in other seed plants.

The seed architecture elucidated here for the charcoalified seeds, which also occurs in extant and fossil Gnetales, Erdtmanithecales and Bennettitales, can be summarized as: seeds orthotropous, with a single integument extended into a long micropylar tube; micropylar canal closed after fertilization by expanded integumentary tissue (or in *Ephedra* by mucilaginous secretion); integument thin, weakly developed; nucellus and megaspore membrane poorly developed or lacking; and integument surrounded by a robust outer envelope comprised in part of sclerenchymatous tissues. The possibility that this seed architecture comprises a synapomorphy, or group of synapomorphies, for a bennettitalean–erdtmanithecalean–gnetalean clade (BEG clade) is also supported by the occurrence of pollen grains with a granular infratectal layer in the pollen wall in all three taxa, and the presence of paracytic stomata in Bennettitales, Erdtmanithecales and *Welwitschia*–*Gnetum*. In the context of current phylogenetic analyses of extant and fossil seed plants, these characters provide further support for some elements of the anthophyte grouping recognized by previous studies[20,22], and most recently in refs 4 and 5 (see also Supplementary Information).

The new evidence presented here links the charcoalified seeds to Gnetales, Erdtmanithecales and Bennettitales, and supports recognition of the BEG clade (Fig. 3). It emphasizes the great diversity of the group from which extant *Ephedra*, *Welwitschia* and *Gnetum* emerged, and the extent to which they are relictual. It also supports earlier ideas of a close relationship between Bennettitales and Gnetales[11,20,23], but in previously unsuspected ways. Testing this hypothesis will need renewed efforts to resolve seed plant phylogeny and to reconcile morphological results with evidence from molecular phylogenetics, which currently conflicts with the anthophyte grouping[24]. Such efforts will also require exploration of the impacts of the trade-off between increased taxon versus increased character sampling on phylogenetic pattern and resolution. Our results also raise the question of how the close similarity among the ovulate structures of Gnetales, Erdtmanithecales and Bennettitales relates to the situation in other seed plants, especially in angiosperms and other possible anthophytes. A next generation of phylogenetic analyses will need to incorporate a greater range of fossil taxa, as well as new kinds of material and character systems, but the consistent occurrence of two layers around the nucellus in the ovules of all three BEG lineages is similar to the typical bitegmic ovules of angiosperms, and is worthy of closer investigation.

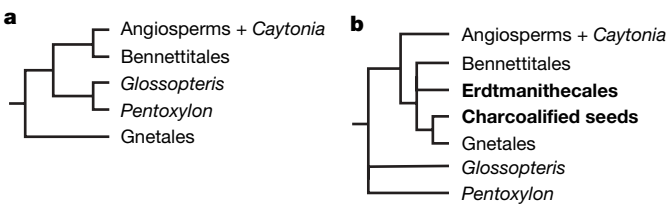

Figure 3 | The phylogenetic relationships among 'anthophytes'. **a**, Topology as for ref. 5, with the Gnetales as the sister clade to the 'higher' seed ferns (*Caytonia*, *Glossopteris* and *Pentoxylon*), Bennettitales and angiosperms. **b**, Topology, under inclusion of the charcoalified seeds and Erdtmanithecales, links the Bennettitales with the Gnetales. For details see Supplementary Information.

METHODS SUMMARY

The fossil seeds were collected at several localities in the Western Portuguese Basin and the Potomac Group of eastern North America, which range in age from late Barremian/early Aptian to mid-Albian. The fossils were extracted from the sediments by sieving in water, and cleaned using established techniques. The seeds were imaged on the X-ray microscope at the TOMCAT beamline of the Swiss Light Source of the Paul Scherrer Institute. We used phase-contrast X-ray tomographic microscopy (PCXTM) to enhance the quality of the tomograms[25,26]. The enhanced contrast of this X-ray imaging technique arises from the phase shift induced in the X-ray wave as it passes through the sample. This method differs from other approaches[27,28] because it couples high resolution and high sensitivity with speed: phase information is obtained by a single tomographic scan. The underlying procedure is based on the assumption of low and homogeneous absorption, but the quality of the resulting images is largely sufficient to perform optimal segmentation and further post-processing. The original algorithm was introduced by Bronnikov[29], further refined by Gureyev *et al.*[30] and implemented experimentally by Groso *et al.*[25].

Full Methods and any associated references are available in the online version of the paper at www.nature.com/nature.

Received 8 July; accepted 19 September 2007.

1. Friis, E. M., Pedersen, K. R. & Crane, P. R. Cretaceous angiosperm flowers: Innovation and evolution in plant reproduction. *Palaeogeogr. Palaeoclimatol. Palaeoecol.* **232,** 251–293 (2006).
2. Pedersen, K. R., Crane, P. R. & Friis, E. M. Pollen organs and seeds with *Eucommiidites* pollen. *Grana* **28,** 279–294 (1989).
3. Rydin, C., Pedersen, K. R., Crane, P. R. & Friis, E. M. Former diversity of *Ephedra* (Gnetales): evidence from Early Cretaceous seeds from Portugal and North America. *Ann. Bot. (Lond.)* **98,** 123–140 (2006).
4. Doyle, J. A. Seed ferns and the origin of angiosperms. *J. Torrey Bot. Soc.* **133,** 169–209 (2006).
5. Hilton, J. & Bateman, R. M. Pteridosperms are the backbone of seed-plant phylogeny. *J. Torrey Bot. Soc.* **133,** 119–168 (2006).
6. Bateman, R. M., Hilton, J. & Rudall, P. J. Morphological and molecular phylogenetic context of the angiosperms: contrasting the 'top-down' and 'bottom-up' approaches used to infer the likely characteristics of the first flowers. *J. Exp. Bot.* **57,** 3471–3503 (2006).
7. Donoghue, P. C. J. *et al.* Synchrotron X-ray tomographic microscopy of fossil embryos. *Nature* **442,** 680–683 (2006).
8. Tafforeau, P. *et al.* Applications of X-ray synchrotron microtomography for non-destructive 3D studies of paleontological specimens. *Appl. Phys. A* **83,** 195–202 (2006).
9. Tafforeau, P., Bentaleb, I., Jaeger, J. J. & Martin, C. Nature of laminations and mineralization in rhinoceros enamel using histology and X-ray synchrotron microtomography: Potential implications for palaeoenvironmental isotopic studies. *Palaeogeogr. Palaeoclimatol. Palaeoecol.* **246,** 206–227 (2007).
10. Friis, E. M., Pedersen, K. R. & Crane, P. R. Angiosperm floral structures from the Early Cretaceous of Portugal. *Plant Syst. Evol.* **8** (suppl.), 31–49 (1994).
11. Thoday, M. G. The female Inflorescence and ovules of *Gnetum africanum*, with notes on *Gnetum scandens. Ann. Bot. (Lond.)* **25,** 1101–1135 (1911).
12. Berridge, E. M. On some points of resemblance between Gnetalean and Bennettitean seeds. *New Phytol.* **10,** 140–144 (1911).
13. Pearson, H. H. W. *Gnetales* (Cambridge Univ. Press, Cambridge, 1929).
14. Martens, P. *Handbuch der Pflanzenanatomie, vol. 12, pt 2:Les gnétophytes* (eds Zimmermann, W., Carlquist, S., Ozenda, P. & Wulff, H. D.) (Gebrüder Borntraeger, Berlin, Stuttgart, 1971).
15. Yang, Y., Geng, B.-Y., Dilcher, D. L., Chen, Z.-D. & Lott, T. A. Morphology and affinities of an Early Cretaceous *Ephedra* (Ephedraceae) from China. *Am. J. Bot.* **92,** 231–241 (2005).
16. Harris, T. M. The fossil flora of Scoresby Sound East Greenland. Part 3: Caytoniales and Bennettitales. *Medd. Grønl.* **85,** 1–133 (1932).
17. Pedersen, K. R., Crane, P. R. & Friis, E. M. Morphology and phylogenetic significance of *Vardekloeftia* Harris (Bennettitales). *Rev. Palaeobot. Palynol.* **60,** 7–24 (1989).
18. Stopes, M. C. New Bennettitean cones from the British Cretaceous. *Phil. Trans. R Soc. B* **208,** 389–440 (1918).
19. Rothwell, G. W. & Stockey, R. A. Anatomically preserved *Cycadeoidea* (Cycadeoidaceae), with a reevaluation of systematic characters for the seed cones of Bennettitales. *Am. J. Bot.* **89,** 1447–1458 (2002).
20. Crane, P. R. Phylogenetic analysis of seed plants and the origin of angiosperms. *Ann. Mo. Bot. Gard.* **72,** 716–793 (1985).
21. Lignier, O. *Végétaux fossiles de Normandie. Structure et affinités du* Bennettites morierei *Sap. & Mar. (sp.)* 1–78 (E. Lanier, Caen, 1894).
22. Doyle, J. A., Donoghue, M. J. & Zimmer, E. A. Integration of morphological and ribosomal RNA data on the origin of angiosperms. *Ann. Mo. Bot. Gard.* **81,** 419–450 (1994).
23. Arber, E. A. N. & Parkin, J. On the origin of angiosperms. *J. Linn. Soc. Bot.* **38,** 29–80 (1907).
24. Burleigh, J. G. & Mathews, S. Phylogenetic signal in nucleotide data from seed plants: implications for resolving the seed plant tree of life. *Am. J. Bot.* **91,** 1599–1613 (2004).
25. Groso, A., Abela, R. & Stampanoni, M. Implementation of a fast method for high resolution phase contrast tomography. *Opt. Express* **14,** 8103–8110 (2006).
26. Bronnikov, A. V. Reconstruction formulas in phase-contrast tomography. *Opt. Commun.* **171,** 239–244 (1999).
27. Cloetens, P. *et al.* Holotomography: Quantitative phase tomography with micrometer resolution using hard synchrotron radiation X rays. *Appl. Phys. Lett.* **75,** 2912–2914 (1999).
28. Weitkamp, T. *et al.* X-ray phase imaging with a grating interferometer. *Opt. Express* **13,** 6296–6304 (2005).
29. Bronnikov, A. V. Theory of quantitative phase-contrast computed tomography. *J. Opt. Soc. Am. A* **19,** 472–480 (2002).
30. Gureyev, T. E., Paganin, D. M., Myers, G. R., Nesterets, Y. I. & Wilkins, S. W. Phase-and-amplitude computer tomography. *Appl. Phys. Lett.* **89,** 034102–1–034102-3 (2006).

Supplementary Information is linked to the online version of the paper at www.nature.com/nature.

Acknowledgements We thank F. Marone of the Swiss Light Source for valuable help in setting up the software on the cluster, and T. Huldtgren and N. J. Gostling for help with data analyses. We also thank the Natural History Museum, London, for the loan of petrified specimens, J.-P. Rioult for information on the Lignier fossils, and J. Hilton for helpful suggestions. This study was funded by the Swiss Light Source (P.C.J.D. and S.B.), European Union FP6, as well as by grants from the Swedish Research Council (E.M.F.), the Carlsberg Foundations (K.R.P. and E.M.F.) and the National Science Foundation (P.R.C.).

Author Information Reprints and permissions information is available at www.nature.com/reprints. Correspondence and requests for materials should be addressed to E.M.F. (else.marie.friis@nrm.se) or M.S. (marco.stampanoni@psi.ch).

METHODS

Geological occurrence and preparation. The fossil seeds were collected from unconsolidated sands and clay at several localities in the Western Portuguese Basin and the Potomac Group of eastern North America. These localities range in age from the late Barremian/early Aptian to the mid-Albian. The fossils were extracted from the sediments by sieving in water. They were then cleaned in HF and HCl, followed by rinsing in water. The two specimens shown here were analysed using PCXTM without further treatment. Other specimens were first studied using scanning electron microscopy (SEM) and then remounted for PCXTM. All specimens for SEM were coated with gold. Nail polish was used as mounting media for both PCXTM and SEM. The fossil material is housed in the palaeobotanical collections of the Swedish Museum of Natural History (S) and the geological collections of the Field Museum, Chicago (PP).

Phase-contrast-enhanced synchrotron-radiation X-ray tomographic microscopy. Standard attenuation-based synchrotron radiation X-ray tomography (SRXTM) has been applied successfully to study various microfossils[7–9], but does not provide sufficient contrast in this fossil material because of the extremely low absorption of the charcoalified cell walls. We used phase-contrast X-ray tomographic microscopy (PCXTM) to enhance the quality of the tomograms[25,26]. The enhanced contrast of this X-ray imaging technique is not dependant on simple attenuation but arises from the phase shift induced in the X-ray wave as it passes through the sample. The method used here differs from other approaches[27,28] because it couples high resolution and high sensitivity with speed. The method yields the three-dimensional distribution of the phase (refractive index) of a weakly absorbing object from a single tomographic scan, minimizing measurement time and delivered dose.

Even though the underlying numerical approach is based on the assumption of low and homogeneous absorption, the quality of the resulting images is largely sufficient to perform optimal segmentation and further post-processing. We provide here a very short mathematical description of the physics underlying this method.

Under the aforementioned assumption, the intensity distribution at distance $z = d$ and angle of rotation θ is approximated by the following simplified 'Transport of Intensity' equation[26]:

$$I_{\theta,z=d}(x,y) = I_{\theta,z=0}(x,y)\left[1 - \frac{\lambda d}{2\pi}\nabla^2\phi_\theta(x,y)\right] \quad (1)$$

where $\phi_\theta(x,y)$ is the phase function of the object. The goal of the method is to reformulate equation (1) to obtain $\delta(x,y,z)$, representing the real part of the complex index of refraction $n = 1 - \delta + i\beta$, from the knowledge of $I_{\theta,z=d}(x,y)$ for $\theta \in [0,\pi]$.

Expressing equation (1) as $\nabla^2\phi_\theta(x,y) = -\frac{2\pi}{\lambda d}g_\theta(x,y)$ with $g_\theta(x,y) = \frac{I_{\theta,z=d}(x,y)}{I_{\theta,z=0}(x,y)} - 1$, applying the 3D Radon transform (denoted by the symbol $\wedge$) and calculating finally the second derivative with respect to the variable $s = x\sin\omega + y\cos\omega$ one gets:

$$\frac{\partial^2}{\partial s^2}\hat{\delta}(s,\theta,\omega) = -\frac{1}{d}\hat{g}_\theta(s,\omega) \quad (2)$$

Expression (2) is a theorem that states that from the 2D Radon transform of the measured value g, one can directly find the 3D Radon transform of δ.

Applying the 3D Radon transform and developing the full derivatives, it can be shown that:

$$\delta(x,y,z) = \frac{1}{4\pi^2 d}\int_0^\pi (q^{**}g_\theta)d\theta \quad (3)$$

where $q(x,y) = \frac{|y|}{x^2+y^2}$ and ** defines the two-dimensional convolution operator.

According to the convolution theorem and taking empirically into account the effects of the, always present, non-zero absorption, equation (3) can be evaluated via Fourier space transformation with the following low-pass filter:

$$q(\xi,\eta) = \frac{|\xi|}{\xi^2 + \eta^2 + \alpha_{\exp}} \quad (4)$$

The values of α_{exp} to be used are found by using a semi-empirical (simulations–experiment) approach which goes beyond the purposes of this article.

We modified Groso's implementation[25] to automatically estimate the factor α_{exp} for each angular projection, optimizing the correction for every angle and therefore enhancing the final quality of the reconstructed slices. Fast Fourier transforms and filtering are done on-the-fly on a 16 nodes Linux cluster during data acquisition. After tomographic reconstruction, the relative values of δ are available: even though this method does not directly provide an absolute value for δ, it definitely delivers images with increased contrast sufficient to perform segmentation.

Slice data. The seeds were imaged using a 10× objective on the X-ray microscope at the TOMCAT beamline of the Swiss Light Source of the Paul Scherrer Institut. Exposure time at 20 keV was 450 ms, and 1,501 projections were acquired equi-angularly over 180°. Projections were post-processed and rearranged into flat- and darkfield-corrected sinograms, and reconstruction was performed on a 32-nodes Linux PC farm. Isotropic voxel dimensions are 0.7 μm. Slice data were analysed and manipulated using AMIRA (www.tgs.com) software for computed tomography.